NIH Public Access
Author Manuscript
Biochemistry. Author manuscript; available in PMC 2009 November 4.

Published in final edited form as:
Biochemistry. 2008 November 4; 47(44): 11415–11423. doi:10.1021/bi800961d.

The histone gene cell cycle regulator HiNF-P is a unique zinc finger transcription factor with a novel conserved auxiliary DNA-binding motif

Ricardo Medina, **Timothy Buck**, **Sayyed K. Zaidi**, **Angela Miele-Chamberland**, **Jane B. Lian**, **Janet L. Stein**, **Andre J. van Wijnen**, and **Gary S. Stein***
Department of Cell Biology and Cancer Center, University of Massachusetts Medical School, Worcester, MA 01655 USA

Abstract

Accumulation of histone proteins is necessary for packaging of replicated DNA during the S-phase of cell cycle. Different mechanisms operate to regulate histone protein levels and induction of human histone gene expression at the G1/S phase transition plays a critical role. The zinc finger HiNF-P and co-activator $p220^{NPAT}$ proteins are key regulators of histone gene expression. Here, we describe a novel HiNF-P-specific conserved region (PSCR) located within the C-terminus that is present in HiNF-P homologs of all metazoan species examined. The PSCR motif is required for activation of histone H4 gene transcription, and contributes to DNA binding of HiNF-P. Thus, the PSCR module represents an auxiliary DNA-binding determinant that plays a critical role in mediating histone gene expression during the cell cycle and defines HiNF-P as a unique cell cycle regulatory member of the zinc finger transcription factor family.

Keywords

cell cycle; histone; HiNF-P; $p220^{NPAT}$; CDK2; cyclin E; S phase; DNA-binding; zinc finger

Histone protein synthesis must be finely coupled to DNA replication to accommodate the newly synthesized DNA during the S-phase of the cell cycle (1,2). Stringent control of histone gene expression is essential for normal cell proliferation and abrogation of histone gene-related cell cycle mechanisms blocks cell growth (3). Multiple levels of regulation operate to ensure that histones are synthesized solely during the period of DNA synthesis. As a consequence of this orchestrated control, accumulation of histone mRNA is observed only when the protein is required. Transcriptional and posttranscriptional mechanisms regulate the level of histone mRNA during this period of the cell cycle. At the G1/S transition phase the histone mRNA synthesis increases three to five fold (4-7). Post-transcriptional mechanisms include cell cycle regulation of the half-life of histone mRNAs (8) and S-phase specific endonucleolytic cleavage of the 3'-end of pre-mRNAs (9,10).

The histone transcription factor HiNF-P is a critical component of a signaling pathway that controls expression of histone H4 genes during the S-phase (11-13). HiNF-P exerts its regulatory function by physically interacting with and controlling the stability of $p220^{NPAT}$ (14,15), a nuclear protein substrate of the cyclin E/CDK2 kinase complex that localizes to specific sub-nuclear foci (16-18). The HiNF-P/$p220^{NPAT}$ activation complex coordinately

* Corresponding Author: Gary S. Stein, Department of Cell Biology and Cancer Center, University of Massachusetts Medical School, 55 Lake Avenue North, Worcester, MA 01655 Tel: (508) 856 5625; Fax: 508−856−6800; Email: Gary.Stein@umassmed.edu.

NIH-PA Author Manuscript
NIH-PA Author Manuscript
NIH-PA Author Manuscript

NIH-PA Author Manuscript

NIH-PA Author Manuscript

NIH-PA Author Manuscript

controls transcription of multiple histone H4 genes that are clustered in the human genome (19-22), and a similar $p220^{NPAT}$-dependent transcriptional mechanism has been proposed for histone H2B and H3 genes (16,17). HiNF-P also recognizes non-histone targets including genes that reinforce the cell cycle regulatory function of HiNF-P (23), as well as the HiNF-P gene itself (24). HiNF-P interacts with several proteins that have functions in transcription and/or RNA processing (25). These key findings together establish that HiNF-P is the end-point effector of a cyclin E/CDK2 signaling cascade that stimulates gene expression at the G1/S phase transition. Limited structure-function studies have been performed to date on this important cell cycle regulatory transcription factor (14,26).

One major structural characteristic of HiNF-P is an N-terminal DNA-binding domain with a tandem array of nine zinc fingers of the C2H2 type (14,26), in which two cysteines and two histidines coordinate a zinc ion to form a characteristic finger-like structure (27). The human genome encodes many zinc finger proteins that specifically control a large number of cellular regulatory pathways. Zinc finger proteins can be distinguished by the presence of auxiliary protein domains that are phylogenetically conserved and may support functional diversity. For example, conserved protein modules associated with zinc finger proteins include the poxvirus and zinc finger (POZ) domain, which is also known as the BTB (Broad-Complex, Tramtrack, and Bric-a-brac) domain (28), the Kruppel-associated box (KRAB) (29) and SCAN domain (named after the four proteins initially found to contain this domain: SRE-ZBP, CTfin51, AW-1 [ZNF174] and Number 18 cDNA or ZnF20) (30).

The POZ/BTB domain is a repressor domain found in the promyelocytic leukemia zinc finger (PLZF) protein involved in embryonic development and hematopoiesis. The KRAB domain is a transcriptional repressor found in transcription factors involved in hematopoietic cell development and differentiation. In contrast to POZ/BTB and KRAB domains, the SCAN domain is not associated with either transcriptional activation or repression. Recently, a new domain has been defined in zinc finger proteins, the SNAG (Snail/GFI-1) domain (31). This repressor domain is present in a variety of proto-oncogenic transcription factors and developmental regulators. Thus, zinc finger associated modules typically support transcriptional repression and are usually located N-terminal to the zinc finger domain. In contrast, HiNF-P functions as an activator and the only non-zinc finger region of the protein is located in the C-terminus and contributes to transactivation (14).

In this study, we describe a new 34 amino acid conserved region (PSCR) in the C-terminus of HiNF-P, immediately adjacent to its zinc finger domain. The PSCR contributes to transcriptional activation of histone H4 gene promoter through the cyclin E/CDK2/$p220^{NPAT}$ pathway. We establish that the PSCR represents an auxiliary DNA-binding determinant and that a single amino acid (Y381) is critical for the DNA-binding activity of HiNF-P. Our findings establish that HiNF-P is a unique member of the zinc finger transcription factor class. Its exquisite conservation throughout metazoan evolution is consistent with retention of a critical cell cycle regulatory role in mediating histone gene expression.

MATERIALS AND METHODS

Cell culture

Human U-2 OS osteosarcoma cells were maintained in McCoy's 5A medium (Invitrogen, Carlsbad, CA) supplemented with 10% fetal bovine serum (FBS), 2 mM L-glutamine, 100 U/ml penicillin G and 100 μg/ml streptomycin. Human HeLa S3 cervical adenocarcinoma cells were maintained in Dulbecco's modified Eagle's medium (DMEM; Invitrogen) supplemented with 10% FBS, 2 mM L-glutamine, 100 U/ml penicillin G and 100 μg/ml streptomycin.

NIH-PA Author Manuscript

NIH-PA Author Manuscript

NIH-PA Author Manuscript

Mutagenesis of HiNF-P

Deletion mutants of HiNF-P were obtained by standard molecular procedures (32). For site-directed mutagenesis mutant oligonucleotides were designed following the instructions provided by the QuickChange Site-Directed Mutagenesis Kit (Stratagene, La Jolla, CA). Reactions were carried out following the manufacturer's instructions using a FLAG-tag HiNF-P plasmid vector as a template. Two independent clones for each mutant construct were selected, full length sequenced and analyzed. All oligonucleotides were gel purified by denaturing polyacrylamide gel electrophoresis. The oligonucleotides used were (in 5' to 3' direction; only top strand shown): ΔPSCR, GTT CAA GTG GCC CCA ACC ACA AGA GG; ΔPSCR1, GTT CAA GTG GCC CGA ACA TGA AGA TGG C, ΔPSCR2, GCT GCA GCT GCT GAC ACA GCA ACT G; ΔPSCR3, CTA CGA GAG TGT AGA GCA ACC ACA AGA GG, ΔPSCR4, CCC GTT TTC GGT ACA AGG TTC GCT ACG; Y381A, GGC ATC CCC GTT TTC GGg caA AGG AAC ATG AAG ATG GCT; Y381F, CAT CCC CGT TTT CGG TtC AAG GAA CAT GAA GAT GG. Underlines and lower case indicate positions for deletion and point mutations, respectively.

Reporter gene assays

Transient transfection of U-2 OS cells with FuGENE6 (Roche, Indianapolis, IN) was carried out in six-well plates seeded at a density of 0.13×10^6 cells per well. The next day, cells were transfected with 200 ng of either a luciferase construct with a minimal promoter sequence containing three HiNF-P binding sites (3X HiNF-P-Luc) or a luciferase construct spanning sites I and II of the histone H4/n gene promoter (H4/n-Luc). Expression vectors for epitope-tagged (FLAG) wild type or mutant HiNF-P proteins (25 or 50 ng), $p220^{NPAT}$ (200 ng) or the corresponding empty vectors (EV) were co-transfected. The total amount of DNA was kept the same in each transfection using the appropriate empty vectors. Cells were harvested 24 h after transfection and cell lysates were measured for luciferase activity, which was normalized to Renilla (phRL-null) activity (dual-luciferase reporter assay system, Promega). Cell lysates (4%) were centrifuged at 16,000g for 15 min at 4 °C and analyzed by western blot as described (see below).

Statistical Analysis

Unless otherwise noted, differences in transcriptional activity in reporter gene assays between empty vector and expression vectors for wild type or mutants HiNF-P and/or $p220^{NPAT}$ were evaluated using general linear mixed models (33). Models were fit by restricted maximum likelihood estimation (34) using the SAS Proc Mixed procedure (35). In the presence of significant differences among means, pairwise comparisons were made using Tukey's HSD test utilizing the estimated covariance matrix to account for correlated observations (36). The distributional characteristics of outcome measures were evaluated by applying the Kolmogorov-Smirnov Goodness of Fit Test for Normality (37) to residuals from fitted linear models and by inspection of frequency histograms of these residuals. Natural logarithms of outcomes were applied to better approximate normally distributed residuals. All computations were performed using the SAS version 9.1.3 (38) and SPSS Version 14 (SPSS Inc., Chicago, IL, 2005) statistical software packages. Results are presented as means ± standard errors transformed back into original units. Statistical significance is defined as present when associated p-values are less than 0.05. Differences with p-values between 0.05 and 0.10 are described as "approaching significance".

Depletion of endogenous HiNF-P by siRNA

For small interfering RNA (siRNA)-mediated knockdown of endogenous HiNF-P mRNA, U-2 OS cells were seeded in six-well plates at a density of 6.2×10^4 cells per well and transfected 24 h later with 25 nM of either *Silencer* Negative Control #1 siRNA (Ambion Inc., Austin,

NIH-PA Author Manuscript

NIH-PA Author Manuscript

NIH-PA Author Manuscript

TX) or 3'UTR HiNF-P-specific double-stranded siRNA oligonucleotides (Ambion Inc.) with Oligofectamine according to the manufacturer's instructions (Invitrogen, Carlsbad, CA). After 24 h of siRNA transfection cells were treated as described for gene reporter assays.

Immunofluorescence microscopy

U-2 OS cells were grown in 6-well plates with coverslips (Fisher Scientific, Springfield, N.J.), seeded at a density of 6×10^4 cells per well. After 24 h transfection cells were prepared for in situ immunofluorescence microscopy. Antibody staining was performed by incubating whole-cell preparations with mouse monoclonal anti-FLAG clone M2 (Sigma, St. Louis, MO) at a 1:5,000 dilution for 1 h at 37°C. The secondary antibody (Alexa 568 goat anti-mouse IgG; Molecular Probes, Eugene, OR) was used at a 1:800 dilution. Immunostaining of cell preparations was captured by an epifluorescence microscope (Zeiss Axioplan II) equipped with a charge-coupled device camera. Digital images were acquired as grayscale and transformed to 8-bit images using MetaMorph software (Molecular Devices, Downingtown, PA). The images were pseudocolored to green using the channel mixer tool of Adobe Photoshop. All images were processed in the same manner.

In vitro coupled transcription/translation and nuclear protein preparation

In vitro transcribed/translated (IVTT) protein was produced by the T_NT Coupled Reticulocyte Lysate System (Promega, Madison, WI). For nuclear extract preparation HeLa cells were seeded at 5×10^5 in 100 mm plates and 24 h later transfected with plasmid DNA (4 μg per plate) using FuGENE6 following the manufacturer's instructions. After 24 h transfection cells were collected and centrifuged at 1,000g for 5 min at 4 °C. All subsequent procedures were done at 4°C. The supernatant was removed and the cell pellet was resuspended in 400 μl of ice-cold lysis buffer (10 mM Tris-HCl pH 7.4, 3 mM $MgCl_2$, 10 mM NaCl, 0.5% NP-40) by gentle pipette mixing. Cells were incubated on ice for 10 min and then centrifugated at 16,000g for 30 seconds. After the supernatant was removed, the pellet was resuspended in 400 μl of ice-cold buffer (10 mM HEPES pH 7.9, 1.5 mM $MgCl_2$, 10 mM KCl). After centrifugation at 4,500g for 1 min, supernatant was carefully removed and the nuclear pellet was resuspended in 100 μl of ice-cold extraction buffer (20 mM HEPES pH 7.9, 1.5 mM $MgCl_2$, 420 mM KCl, 0.2 mM EDTA, 20% glycerol). Nuclei were incubated with constant agitation at 4 °C for 45 min. Nuclear extracts were recovered by centrifugation at 16,000g for 5 min and snap frozen in liquid nitrogen and kept at −80° C until use. Protein content was quantified by Bradford assay (Pierce, Rockford, IL).

Western blotting analysis

Nuclear extracts or IVTT-produced proteins were loaded onto 10% sodium dodecyl sulfate (SDS)-polyacrylamide gels and transferred to a polyvinylidene fluoride (PVDF) Immobilon-P membrane (Millipore, Billerica, MA) for 30 min at 10 V in a semi-dry transfer apparatus (model HEP-1, Owl Separation Systems, Portsmouth, NH). Immunodetection was performed using an appropriate dilution of specific antibodies with the Western Lightning Chemiluminescence Reagent Plus assay (Perkin Elmer Life Sciences, Waltham, MA). The following dilutions of primary antibodies were used: rabbit polyclonal CDK2 1:5,000 (M-2, sc163; Santa Cruz Biotechnology Inc., Santa Cruz, CA); mouse monoclonal FLAG 1:5,000 (M2, Sigma); and rabbit polyclonal HiNF-P 1:2,000.

Electrophoretic mobility shift assay

Binding of wild type or mutant HiNF-P proteins to a specified double strand oligonucleotide was assessed either with nuclear extracts overexpressing FLAG-tag or with IVTT-produced proteins. In vitro DNA binding reactions were performed by combining 2 to 5 μg of nuclear extracts or 1 to 8 μl of IVTT-produced protein in a total volume of 9 μl of protein buffer (final

NIH-PA Author Manuscript

NIH-PA Author Manuscript

NIH-PA Author Manuscript

concentrations of 9 mM HEPES pH 7.5, 0.09 mM EDTA pH 8.0, 50 mM KCl, 10% glycerol, 1X Complete protease inhibitor [Roche, Indianapolis, IN], 1 mM NaF, and 1 mM Na_3VO_4) with 10 μl of a DNA mixture containing 10 to 20 fmol of labeled, double stranded oligonucleotide in DNA buffer (final concentrations of 0.1 μg/μl of Salmon sperm DNA, 1 mM DTT, 0.5 mM $MgCl_2$, 0.1 mM $ZnCl_2$). Where indicated, unlabeled oligonucleotide competitor (in 1 μl) was added in 100-fold molar excess. Mixtures were incubated for 20 min at room temperature, and the protein/DNA complexes were then separated in 4% (40:1) native polyacrylamide gels using 1X TBE as running buffer at 4°C. Gels were dried and exposed to BioMax XAR or MR (Kodak, New Haven, CT) films at −80°C. Oligonucleotides used were (in 5' to 3' direction): an optimized HiNF-P binding site based on its recognition sequence in Site II of the H4/n gene, CTT CAG GTT TTC AAT CTG GTC CGA TAC T; HiNF-P mutant, CTT CAG GTT TTC AAT CTT CTA CGA TAC T (mutated nucleotides are underlined) and as non-specific competitor, ATT CGA TCG GGG CGG GGC GAG C.

Sequence alignment and 3D modeling

Multiple sequence alignment to obtain structure-function information of PSCR motifs among HiNF-P homologs was done using ClustalW and GeneDoc softwares (39). Three-dimensional modeling of the PSCR motif was performed using 3D-Phyre software (40,41).

RESULTS

A conserved C-terminal domain in HiNF-P contributes to histone H4 gene transcriptional activation by the HiNF-P/p220^{NPAT} complex

The histone H4 transcription factor HiNF-P has an N-terminal domain containing 9 zinc fingers and a C-terminal region with unknown function. Several zinc finger transcription factors have conserved motifs outside the zinc finger domain (e.g., POZ/BTB, KRAB, SCAN and SNAG domains) (31,42). Similarly, sequence alignment analysis reveals that the transcription factor HiNF-P possesses an evolutionary conserved sequence of 34 amino acids in its C-terminal region (HiNF-P Specific Conserved Region, PSCR; aa 374 to 407) (see Fig. 6 below). To address whether this conserved region has a role in HiNF-P/p220^{NPAT}-dependent activation of histone H4 gene transcription, we constructed a series of HiNF-P mutants with external and internal deletions in the C-terminus. Wild type HiNF-P and p220^{NPAT} synergize to produce a 14-fold induction of a luciferase reporter controlled by a multimerized HiNF-P recognition site in U-2 OS cells, while transfection of p220^{NPAT} alone produces only a 4.5-fold induction (Fig. 1A), consistent with previous findings (14). Deletion of the C-terminus of HiNF-P to either amino acid 452 or 395 in each case abolishes co-activation of the HiNF-P responsive promoter in U-2 OS cells in the presence of p220^{NPAT}(Fig. 1B). These results suggest that the C-terminus of HiNF-P between amino acid 452 and 517 contributes to transcriptional activation. Strikingly, internal deletion of the PSCR completely abolishes HiNF-P/p220^{NPAT} co-activation of the multimerized histone H4 promoter (Fig. 1C). To further characterize the PSCR, we generated three additional internal deletions within the PSCR. Deletion of aa 374−382 (ΔPSCR1), but neither aa 394−400 nor 401−407 (i.e., mutants ΔPSCR2 and ΔPSCR3) of HiNF-P, abrogates transcriptional co-activation of the HiNF-P responsive promoter (Fig. 1C). Thus, these results establish that the PSCR of HiNF-P is required for synergistic activation of histone H4 gene transcription together with p220^{NPAT}.

We tested whether the PSCR is required for transcriptional activation of the native histone H4 gene promoter by the HiNF-P/p220^{NPAT} complex (Fig. 2). To increase sensitivity of reporter gene expression to exogenous wild type and mutants HiNF-P, we depleted endogenous HiNF-P levels using a siRNA approach. We selected a HiNF-P siRNA that specifically targets the 3'-UTR of the native HiNF-P mRNA, but does not affect exogenously expressed HiNF-P because our expression constructs lack these 3'-UTR sequences. The HiNF-P siRNA

NIH-PA Author Manuscript

NIH-PA Author Manuscript

NIH-PA Author Manuscript

oligonucleotide treatment was initiated 24 hours prior to transfections with plasmid vectors. The histone H4 gene promoter is only activated by $p220^{NPAT}$ when HiNF-P levels are not depleted by siRNA (Fig. 2A), corroborating our previous results (14). Exogenous expression of wild type HiNF-P restores $p220^{NPAT}$ activation (Figs. 2A and 2B), while the HiNF-P mutant ΔPSCR (aa 374−407) does not (Fig. 2B). Hence, the PSCR is required for the transmission of signals from the cyclin E/CDK2/$p220^{NPAT}$ pathway that stimulate transcription of the cell cycle regulated native histone H4 gene promoter.

The PSCR motif represents an auxiliary DNA-binding determinant

To ensure that the exogenous wild type and mutant HiNF-P proteins are properly directed to the nucleus, we performed immunofluorescence (IF) microscopy and electrophoretic mobility shift assays (EMSAs) with nuclear lysates. Wild type HiNF-P as well as external (aa 1−452 and aa 1−395) and internal deletions encompassing the PSCR sequences (ΔPSCR, ΔPSCR1, ΔPSCR2 and ΔPSCR3) are all localized to the nucleus (Fig. 3). This finding demonstrates that loss of transcriptional co-activation upon deletion of the PSCR motif of HiNF-P is not due to sub-cellular mislocalization but reinforces the idea that this conserved region is important for HiNF-P function. Our data also indicate that a nuclear localization signal is present in the N-terminal zinc finger region of HiNF-P between amino acids 1 to 395.

Wild type HiNF-P forms a characteristic HiNF-P/DNA complex in EMSAs that is effectively competed by an unlabeled wild type oligonucleotide but not by the corresponding mutant oligonucleotide (Fig. 4A, lanes 2−4). When we examined the levels of HiNF-P mutants in nuclear lysates using EMSAs, we did not observe the expected protein/DNA complex for the ΔPSCR mutant (Fig. 4A, lane 5). However, IF data (Fig. 3) and western blot data (Fig. 4A, lower panel) clearly indicate the presence of this mutant protein in the nucleus.

To examine whether this protein may have lost the ability to bind the HiNF-P recognition motif, we performed EMSAs with recombinant HiNF-P proteins that where produced by coupled in vitro transcription/translation (Fig. 4B and Fig. 4C). Recombinant wild type and mutant proteins were all produced at the same levels, as demonstrated by western blot analysis (Fig. 4C, lower panel). The external deletion mutants 1−452 and 1−395 are both capable of sequence-specific binding to the histone H4 gene promoter in vitro, albeit that the 1−395 mutant exhibits slightly decreased binding (Fig. 4B, lane 8). Strikingly, the recombinant ΔPSCR mutant protein does not bind to the HiNF-P probe (Fig. 4C, lane 2). Therefore, we also monitored binding of four additional internal deletion mutants of the PSCR region. Removal of aa 394−400 or 401−407 (i.e., mutants ΔPSCR2 and ΔPSCR3) does not affect DNA-binding (Fig. 4C, lanes 5 and 6), but deletion of either aa 374−382 or 383−393 (i.e., mutants ΔPSCR1 and ΔPSCR4) of HiNF-P abolishes DNA-binding activity (Fig. 4C, lanes 3 and 4). The loss of binding of ΔPSCR4 (Fig. 4C, lane 4) is consistent with the decreased protein/DNA interaction observed for the 1−395 deletion, which is apparently truncated near amino acids of HiNF-P required for DNA binding (see Fig. 4B, lane 8). Taken together, these findings establish that the N-terminal segment (aa 374−393) of the PSCR motif is required for DNA-binding of HiNF-P and thus represents an auxiliary DNA-binding determinant.

To test whether HiNF-P mutants still retain their ability to interact with $p220^{NPAT}$, we performed EMSAs to detect the ternary complex, $p220^{NPAT}$/HiNF-P/DNA (Fig. 4D). We used recombinant HiNF-P proteins and a truncated $p220^{NPAT}$ protein corresponding to aa 1−499 that we have previously shown interacts functionally with HiNF-P (14). In the presence of $p220^{NPAT}$, full length HiNF-P forms a ternary complex that is detected in EMSA as a band of reduced mobility (Fig.4D, lane 3) and is specifically competed by HiNF-P oligonucleotide (Fig. 4D, lane 4). We monitored the interaction of all four HiNF-P deletion mutants which still retain their ability to bind DNA. External deletion mutants 1−452 and 1−395 as well as internal deletions ΔPSCR2 and ΔPSCR3 (aa 394−400 and 401−407, respectively) still form a ternary

NIH-PA Author Manuscript

NIH-PA Author Manuscript

NIH-PA Author Manuscript

complex with $p220^{NPAT}$. These results suggest that the C-terminal portion of HiNF-P beyond aa 395 is not required for $p220^{NPAT}$ interaction.

A single point mutation within the PSCR motif abolishes DNA-binding activity of HiNF-P

The N-terminal segment of the PSCR is composed of 34 conserved amino acids (SGHPR FRYKE HEDGY MRLQL VRYES VELTQ QLLR). We generated four separate alanine substitutions (S374A, Y381A, K382A and Y388A) that were tested for DNA-binding activity in EMSAs as recombinant proteins or in nuclear extracts (Fig. 5 and data not shown). All proteins produced by IVTT or in transient transfections were expressed at similar levels by western blot analysis (Fig. 5B, lower panel and data not shown). The HiNF-P point mutants are present in the nucleus as demonstrated by immunofluorescence microscopy (Fig. 5A and data not shown). Mutation of S374, K382A or Y388A does not significantly affect DNA-binding (data not shown). However, alanine mutation of Y381 abolishes the interaction of HiNF-P with its cognate site (Fig. 5B, lane 7). In contrast, mutation of Y381 to phenylalanine (mutant Y381F) does not abolish the DNA-binding activity of HiNF-P (Fig. 5B, lane 8). The differences in DNA-binding activity of the Y381A and Y381F point mutants is directly reflected by differences in their transactivation potential on the histone H4 gene promoter (Fig. 5C). Our data establish that tyrosine 381 is critical for HiNF-P DNA-binding and corroborate the conclusion that the PSCR motif contributes to the ability of HiNF-P to recognize its cognate cell cycle regulatory element. Three dimensional modeling of the PSCR motif suggests that this segment of HiNF-P has the potential to form a beta hairpin-alpha helix structure that is perhaps analogous to the zinc-stabilized beta strand-alpha helix structure typically observed in zinc finger modules (Fig. 6).

DISCUSSION

Previous studies revealed that the human histone H4 transcription factor HiNF-P contains nine N-terminal zinc fingers and that its C-terminus contributes to transcriptional activation of histone H4 genes (14). Here, we show that HiNF-P contains a highly conserved 34 amino acid region (PSCR) within the C-terminus that represents an auxiliary DNA-binding determinant. Experimental data and molecular modeling of the PSCR suggest that there are two distinct peptides (aa 374−393 and aa 394−407). While the 394−407 peptide is dispensable for DNA-binding, the 374−393 peptide is required and a point mutation of a conserved tyrosine residue (Y381) is sufficient to abolish sequence-specific binding to and activation of the histone H4 gene promoter.

The identification of the PSCR domain defines HiNF-P as a unique member of the zinc finger transcription factor family that is distinct from four major subgroups of zinc finger proteins that have been described in other studies. Many zinc finger proteins contain an auxiliary module that is typically located in the N-terminus of the protein, including the POZ/BTB (28), KRAB (29), SCAN (30), and SNAG domains (31). Unlike the PSCR domain, the POZ/BTB, KRAB and SNAG modules have all been characterized as repressor domains, while the SCAN domain contributes to transcriptional control through dimerization. In contrast to these motifs, that are all involved in protein-protein interactions, one important function of the PSCR region is to facilitate DNA-binding of HiNF-P to support its critical role in cell cycle-dependent activation of the histone H4 gene promoter.

Histones are encoded by a multigene family and are essential for chromatin structure and cell viability in species from yeast to man. While the zinc finger region of HiNF-P exhibits similarity with a large number of mammalian transcription factors, the PSCR is not present in any other protein encoded by the human genome. This observation indicates that HiNF-P is a singular member of the zinc finger protein family that is at least in part dedicated to histone gene expression. Although there is no paralog for HiNF-P in the human genome, the PSCR is

NIH-PA Author Manuscript

NIH-PA Author Manuscript

NIH-PA Author Manuscript

highly conserved in putative homologs of HiNF-P in all metazoan species for which sequence information is available. The conservation of the PSCR motif suggests that the regulatory function of HiNF-P originated early during evolution of multicellular species.

In conclusion, our data demonstrate that the C-terminus of HiNF-P contains a novel protein segment that is critical for the cell cycle regulatory function of HiNF-P in activation of histone gene expression. The unique nature of this protein segment may permit the development of inhibitory molecules that will block HiNF-P function as a potential strategy for intervening in deregulated proliferation of cancer cells.

ACKNOWLEDGMENTS

We thank Judy Rask for expert assistance in the preparation of this manuscript and Stephen Baker for expert advice with statistical analysis. We also thank the members of our research group and especially Rong-Lin Xie and Margaretha van der Deen for stimulating discussions.

Grant Support: These studies were supported by NIH grant GM032010. The contents of this manuscript are solely the responsibility of the authors and do not necessarily represent the official views of the National Institutes of Health.

Abbreviations

PSCR, HiNF-P specific conserved region; aa, amino acid; UTR, untranslated region; CDK, cyclin-dependent kinase; SDS, sodium dodecyl sulfate; DTT, dithiothreitol.

REFERENCES

1. Stein GS, Stein JL, van Wijnen AJ, Lian JB. Regulation of histone gene expression. Curr. Opin. Cell Biol 1992;4:166–173. [PubMed: 1599687]
2. Stein GS, van Wijnen AJ, Stein JL, Lian JB, Montecino M, Zaidi SK, Braastad C. An architectural perspective of cell-cycle control at the G1/S phase cell-cycle transition. J Cell Physiol 2006;209:706–710. [PubMed: 17001681]
3. Ye X, Wei Y, Nalepa G, Harper JW. The cyclin E/Cdk2 substrate p220(NPAT) is required for S-phase entry, histone gene expression, and Cajal body maintenance in human somatic cells. Mol. Cell Biol 2003;23:8586–8600. [PubMed: 14612403]
4. Plumb M, Stein J, Stein G. Coordinate regulation of multiple histone mRNAs during the cell cycle in HeLa cells. Nucl. Acids Res 1983;11:2391–2410. [PubMed: 6304651]
5. Baumbach LL, Stein GS, Stein JL. Regulation of human histone gene expression: transcriptional and posttranscriptional control in the coupling of histone messenger RNA stability with DNA replication. Biochemistry 1987;26:6178–6187. [PubMed: 3689769]
6. Heintz N, Sive HL, Roeder RG. Regulation of human histone gene expression: kinetics of accumulation and changes in the rate of synthesis and in the half-lives of individual histone mRNAs during the HeLa cell cycle. Mol. Cell Biol 1983;3:539–550. [PubMed: 6406835]
7. Harris ME, Bohni R, Schneiderman MH, Ramamurthy L, Schumperli D, Marzluff WF. Regulation of histone mRNA in the unperturbed cell cycle: evidence suggesting control at two posttranscriptional steps. Mol. Cell Biol 1991;11:2416–2424. [PubMed: 2017161]
8. Morris TD, Weber LA, Hickey E, Stein GS, Stein JL. Changes in the stability of a human H3 histone mRNA during the HeLa cell cycle. Mol. Cell. Biol 1991;11:544–553. [PubMed: 1986245]
9. Dominski Z, Marzluff WF. Formation of the 3' end of histone mRNA. Gene 1999;239:1–14. [PubMed: 10571029]
10. Dominski Z, Marzluff WF. Formation of the 3' end of histone mRNA: getting closer to the end. Gene 2007;396:373–390. [PubMed: 17531405]
11. van Wijnen AJ, van den Ent FM, Lian JB, Stein JL, Stein GS. Overlapping and CpG methylation-sensitive protein-DNA interactions at the histone H4 transcriptional cell cycle domain: distinctions between two human H4 gene promoters. Mol. Cell. Biol 1992;12:3273–3287. [PubMed: 1620129]

NIH-PA Author Manuscript NIH-PA Author Manuscript NIH-PA Author Manuscript

12. Mitra P, Xie RL, Medina R, Hovhannisyan H, Zaidi SK, Wei Y, Harper JW, Stein JL, van Wijnen AJ, Stein GS. Identification of HiNF-P, a key activator of cell cycle controlled histone H4 genes at the onset of S phase. Mol. Cell. Biol 2003;23:8110–8123. [PubMed: 14585971]
13. Mitra P, Xie R, Harper JW, Stein JL, Stein GS, van Wijnen AJ. HiNF-P is a bifunctional regulator of cell cycle controlled histone H4 gene transcription. J. Cell. Biochem 2007;101:181–191. [PubMed: 17163457]
14. Miele A, Braastad CD, Holmes WF, Mitra P, Medina R, Xie R, Zaidi SK, Ye X, Wei Y, Harper JW, van Wijnen AJ, Stein JL, Stein GS. HiNF-P directly links the cyclin E/CDK1/p220^{NPAT} pathway to histone H4 gene regulation at the G1/S phase cell cycle transition. Mol. Cell. Biol 2005;25:6140–6153. [PubMed: 15988025]
15. Medina R, van Wijnen AJ, Stein GS, Stein JL. The histone gene transcription factor HiNF-P stabilizes its cell cycle regulatory co-activator p220^{NPAT}. Biochemistry 2006;45:15915–15920. [PubMed: 17176114]
16. Zhao J, Kennedy BK, Lawrence BD, Barbie DA, Matera AG, Fletcher JA, Harlow E. NPAT links cyclin E-Cdk2 to the regulation of replication-dependent histone gene transcription. Genes Dev 2000;14:2283–2297. [PubMed: 10995386]
17. Ma T, Van Tine BA, Wei Y, Garrett MD, Nelson D, Adams PD, Wang J, Qin J, Chow LT, Harper JW. Cell cycle-regulated phosphorylation of p220(NPAT) by cyclin E/Cdk2 in Cajal bodies promotes histone gene transcription. Genes Dev 2000;14:2298–2313. [PubMed: 10995387]
18. Ghule PN, Becker KA, Harper JW, Lian JB, Stein JL, van Wijnen AJ, Stein GS. Cell cycle dependent phosphorylation and subnuclear organization of the histone gene regulator p220^{NPAT} in human embryonic stem cells. J. Cell. Physiol 2007;213:9–17. [PubMed: 17520687]
19. Holmes WF, Braastad CD, Mitra P, Hampe C, Doenecke D, Albig W, Stein JL, van Wijnen AJ, Stein GS. Coordinate control and selective expression of the full complement of replication-dependent histone H4 genes in normal and cancer cells. J. Biol. Chem 2005;280:37400–37407. [PubMed: 16131487]
20. Braastad CD, Hovhannisyan H, van Wijnen AJ, Stein JL, Stein GS. Functional characterization of a human histone gene cluster duplication. Gene 2004;342:35–40. [PubMed: 15527963]
21. Becker KA, Stein JL, Lian JB, van Wijnen AJ, Stein GS. Establishment of histone gene regulation and cell cycle checkpoint control in human embryonic stem cells. J Cell Physiol 2007;210:517–526. [PubMed: 17096384]
22. Doenecke D, Albig W, Bode C, Drabent B, Franke K, Gavenis K, Witt O. Histones: genetic diversity and tissue-specific gene expression. Histochem. Cell Biol 1997;107:1–10. [PubMed: 9049636]
23. Medina R, van der Deen M, Miele-Chamberland A, Xie RL, van Wijnen AJ, Stein JL, Stein GS. The HiNF-P/p220^{NPAT} cell cycle signaling pathway controls non-histone target genes. Cancer Res 2007;67:10334–10342. [PubMed: 17974976]
24. Xie RL, Liu L, Mitra P, Stein JL, van Wijnen AJ, Stein GS. Transcriptional activation of the histone nuclear factor P (HiNF-P) gene by HiNF-P and its cyclin E/CDK2 responsive co-factor p220(NPAT) defines a novel autoregulatory loop at the G1/S phase transition. Gene 2007;402:94–102. [PubMed: 17826007]
25. Miele A, Medina R, van Wijnen AJ, Stein GS, Stein JL. The interactome of the histone gene regulatory factor HiNF-P suggests novel cell cycle related roles in transcriptional control and RNA processing. J. Cell. Biochem 2007;102:136–148. [PubMed: 17577209]
26. Sekimata M, Homma Y. Sequence-specific transcriptional repression by an MBD2-interacting zinc finger protein MIZF. Nucleic Acids Res 2004;32:590–597. [PubMed: 14752047]
27. Huntley S, Baggott DM, Hamilton AT, Tran-Gyamfi M, Yang S, Kim J, Gordon L, Branscomb E, Stubbs L. A comprehensive catalog of human KRAB-associated zinc finger genes: insights into the evolutionary history of a large family of transcriptional repressors. Genome Res 2006;16:669–677. [PubMed: 16606702]
28. Bardwell VJ, Treisman R. The POZ domain: a conserved protein-protein interaction motif. Genes Dev 1994;8:1664–1677. [PubMed: 7958847]
29. Bellefroid EJ, Poncelet DA, Lecocq PJ, Revelant O, Martial JA. The evolutionarily conserved Kruppel-associated box domain defines a subfamily of eukaryotic multifingered proteins. Proc. Natl. Acad. Sci. U. S. A 1991;88:3608–3612. [PubMed: 2023909]

NIH-PA Author Manuscript

NIH-PA Author Manuscript

NIH-PA Author Manuscript

30. Williams AJ, Khachigian LM, Shows T, Collins T. Isolation and characterization of a novel zinc-finger protein with transcription repressor activity. J. Biol. Chem 1995;270:22143–22152. [PubMed: 7673192]

31. Grimes HL, Chan TO, Zweidler-McKay PA, Tong B, Tsichlis PN. The Gfi-1 proto-oncoprotein contains a novel transcriptional repressor domain, SNAG, and inhibits G1 arrest induced by interleukin-2 withdrawal. Mol. Cell Biol 1996;16:6263–6272. [PubMed: 8887656]

32. Sambrook, J.; Russell, DW. Molecular Cloning: A Laboratory Manual. Cold Spring Harbor Laboratory Press; Cold Spring Harbor: 2001.

33. McLean RA, Sanders WL, Stroup WW. A unified approach to mixed linear models. The American Statistician 1991;45:54–64.

34. Corbeil RR, Searle SR. Restricted maximum likelihood (REML) estimation of variance components in the mixed model. Technometrics 1976;18:31–38.

35. SAS Institute Inc.. The MIXED Procedure. SAS/STAT Software: Changes and Enhancements through Release 6.12. SAS Institute, Inc.; Cary, NC: 1997.

36. Hsu JC. The factor analytic approach to simultaneous inference in the general linear model. J. Computational and Graphical Statistics 1992;1:168.

37. Daniel, WW. Applied Nonparametric Statistics. Duxbury Press; Pacific Grove, CA: 1990.

38. SAS Institute Inc.. Base SAS 9.1.3 Procedures Guide. SAS Institute Inc.; Gary, NC: 2006.

39. Nicholas KB, Nicholas HB Jr. Deerfield DW II. GeneDoc: analysis and visualization of genetic variation. EMBNEW. NEWS 1997;4:14.

40. Bennett-Lovsey RM, Herbert AD, Sternberg MJ, Kelley LA. Exploring the extremes of sequence/structure space with ensemble fold recognition in the program Phyre. Proteins 2008;70:611–625. [PubMed: 17876813]

41. Kelley LA, MacCallum RM, Sternberg MJ. Enhanced genome annotation using structural profiles in the program 3D-PSSM. J. Mol. Biol 2000;299:499–520. [PubMed: 10860755]

42. Collins T, Stone JR, Williams AJ. All in the family: the BTB/POZ, KRAB, and SCAN domains. Mol. Cell Biol 2001;21:3609–3615. [PubMed: 11340155]

NIH-PA Author Manuscript

NIH-PA Author Manuscript

NIH-PA Author Manuscript

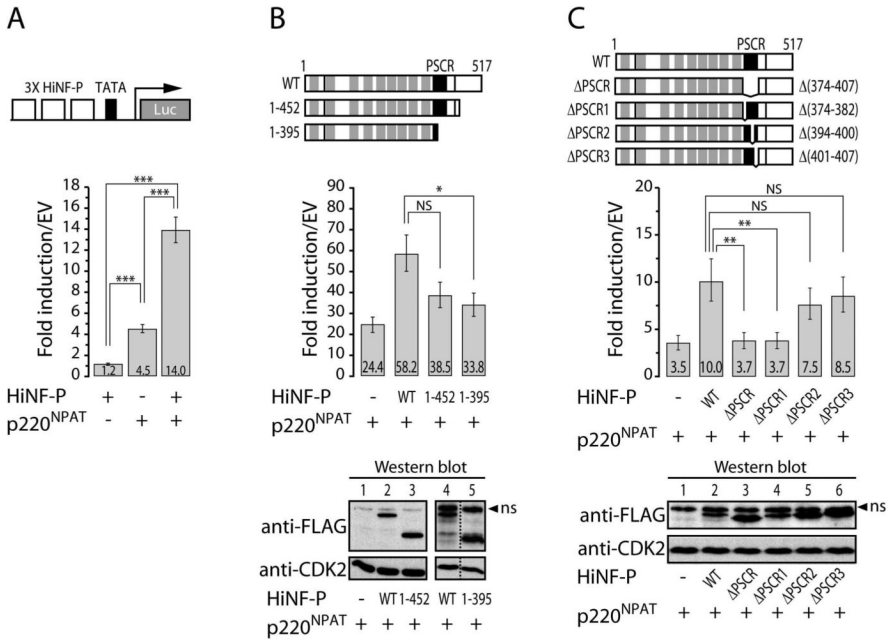

Figure 1. HiNF-P and p220^{NPAT} co-activation of a multimerized promoter requires the PSCR motif located at the C-terminus of HiNF-P

U-2 OS cells were transfected with a multimerized HiNF-P binding site fused to a minimal TATA box promoter-luciferase construct (3X HiNF-P-Luc) together with wild type or mutant HiNF-P and p220^{NPAT} proteins. (A) Expression of p220^{NPAT} alone results in a 4.5-fold activation and co-expression of HiNF-P and p220^{NPAT} elevates the promoter activity by 14.0-fold. (B) Progressive external deletion of the C-terminal region of HiNF-P abolishes the co-activation of promoter activity induced by co-transfection of wild type HiNF-P and p220^{NPAT}. Both deletion mutants, aa 1−452 and aa 1−395, show basal transcriptional levels similar to that achieved by transfection with p220^{NPAT} alone, although only mutant 1−395 attains statistical significance. The top portion shows a diagram of wild type (WT) and HiNF-P mutant proteins. Depicted are the zinc finger motif (gray boxes), HiNF-P specific conserved region (PSCR; black box) and two acidic regions (black lines). The lower panel shows similar protein levels for wild type (WT) and external deletion mutant HiNF-P proteins from the indicated luciferase samples detected by western blot using FLAG antibody (CDK2 is shown as loading control; ns: non-specific). (C) Internal deletion of the PSCR motif (ΔPSCR; aa 374 to 407) as well as deletion of aa 374 to 382 (ΔPSCR1), but neither aa 394−400 nor 401−407 (i.e., mutants ΔPSCR2 and ΔPSCR3) of HiNF-P, abolishes transcriptional co-activation of the HiNF-P responsive promoter. The top portion shows a diagram of wild type (WT) and HiNF-P mutant proteins. The lower panel shows similar protein levels for wild type (WT) and internal deletion mutant HiNF-P proteins from the indicated luciferase samples detected by western blot using FLAG antibody (CDK2 is shown as loading control; ns: non-specific).
Results are presented as mean ± standard error. NS: not significant, †: 0.05<p<0.1, *: p<0.05, **: p<0.01 and ***: p<0.001.

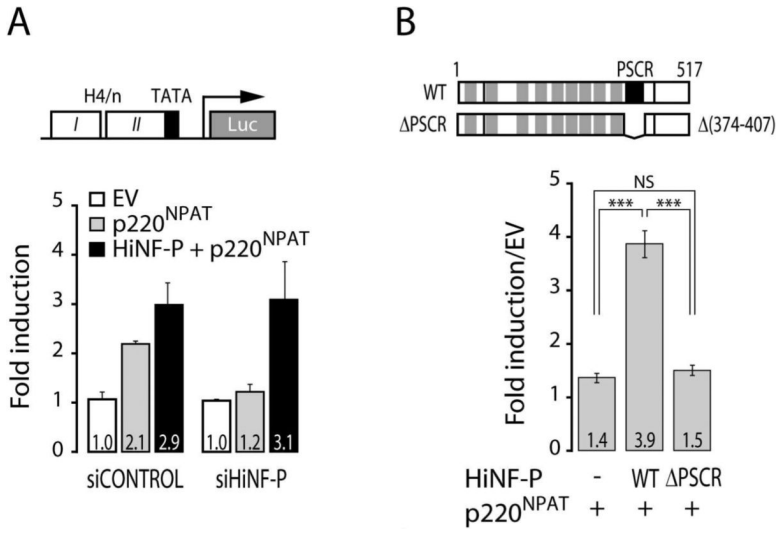

Figure 2. The PSCR motif of HiNF-P is required for the co-activation of the wild type histone H4 gene promoter

U-2 OS cells were transfected with the wild type histone H4/n gene promoter-luciferase reporter construct (H4/n-Luc) together with wild type or mutant HiNF-P and p220^{NPAT} proteins. (A) Depletion of endogenous HiNF-P by siRNA abolishes p220^{NPAT} co-activation. Cells were transfected with control siRNA (siCONTROL) or 3'-UTR-specific HiNF-P siRNA (siHiNF-P) oligonucleotides for 24 h followed by transfection with a H4/n-Luc construct together with empty vector or expression vectors for HiNF-P and p220^{NPAT} for 24 h. Transfection with p220^{NPAT} alone produces a 2.1-fold activation of the reporter construct in siCONTROL-treated cells, but returns to basal transcriptional activity levels when cells are depleted of HiNF-P (siHiNF-P). Transfection of exogenous HiNF-P together with p220^{NPAT} in HiNF-P-depleted cells (siHiNF-P) re-establishes the co-activation observed in control-treated cells (siCONTROL). Results are presented as means ± standard deviation. (B) HiNF-P and p220^{NPAT} co-activation of the wild type histone H4 gene promoter requires the PSCR motif of HiNF-P. U-2 OS cells were treated with a 3'-UTR-specific HiNF-P siRNA oligonucleotide (25 nM) for 24 h as above and transfected with a H4/n-Luc construct together with expression vectors for wild type HiNF-P (WT), mutant ΔPSCR HiNF-P and p220^{NPAT} proteins for 24 h. Transcriptional basal levels are observed in HiNF-P-depleted U-2 OS cells when p220^{NPAT} is transfected alone. Transfection of exogenous wild type HiNF-P together with p220^{NPAT} produces a 3.9-fold co-activation; however transfection of mutant ΔPSCR together with p220^{NPAT} abolishes this co-activation. Results are presented as mean ± standard error. NS: not significant, †: 0.05<p<0.1, *: p<0.05, **: p<0.01 and ***: p<0.001. Top panel shows a diagram of wild type (WT) and mutant ΔPSCR HiNF-P proteins; deleted amino acids are indicated at the right (for further details see Fig. 1B).

NIH-PA Author Manuscript NIH-PA Author Manuscript NIH-PA Author Manuscript

NIH-PA Author Manuscript
NIH-PA Author Manuscript
NIH-PA Author Manuscript

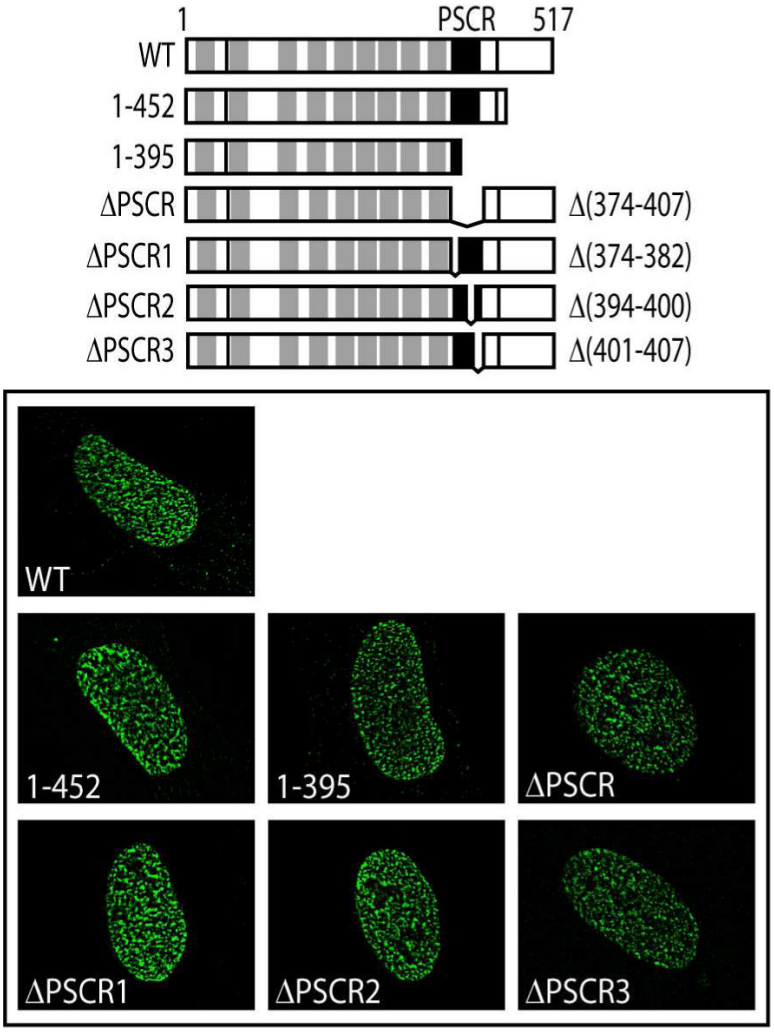

Figure 3. Sub-cellular localization of wild type and mutant HiNF-P proteins

Human U-2 OS cells were grown on coverslips, transfected with FLAG-tagged proteins and analyzed by in situ immunofluorescence microscopy. Wild type and mutant HiNF-P proteins (see diagram) were detected using a mouse monoclonal FLAG (M2) antibody. Wild type, as well as external (1−452 and 1−395) and internal (ΔPSCR, ΔPSCR1, ΔPSCR2 and ΔPSCR3) deletion HiNF-P proteins show characteristic nuclear staining.

NIH-PA Author Manuscript
NIH-PA Author Manuscript
NIH-PA Author Manuscript

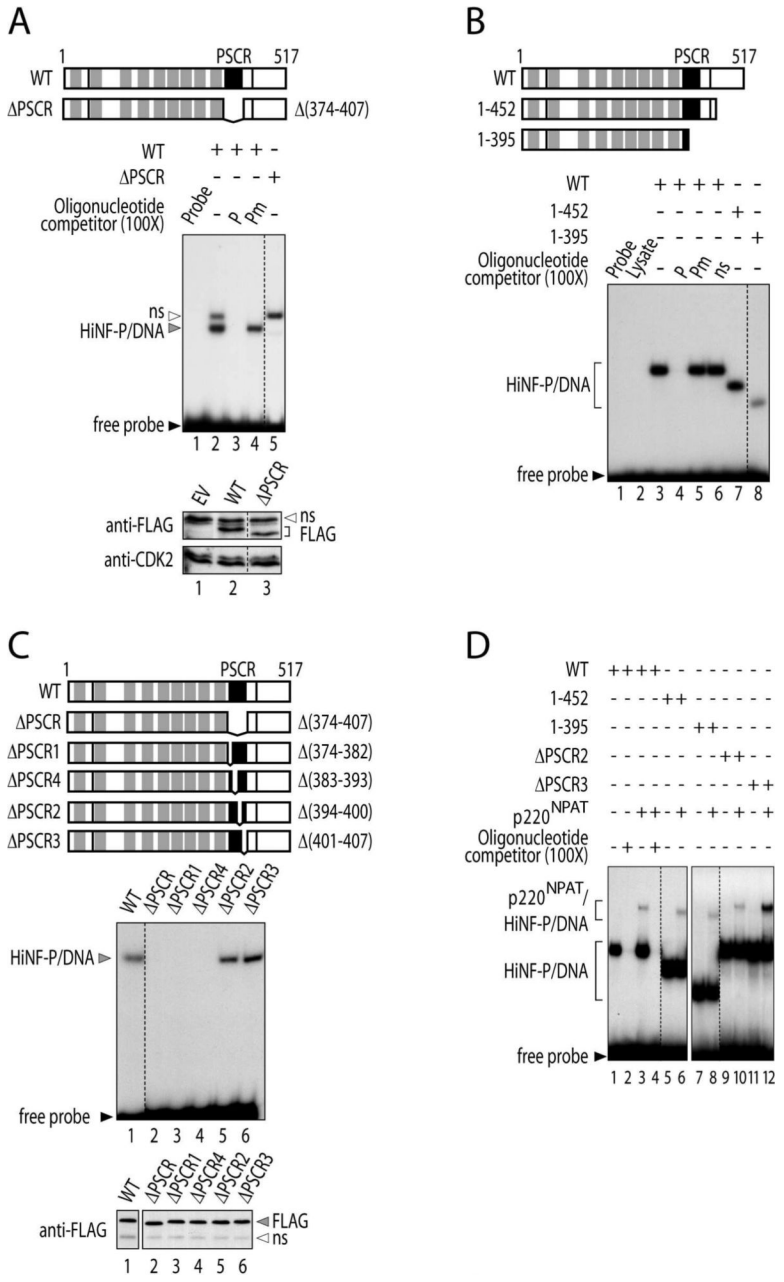

Figure 4. The PSCR domain of HiNF-P is an auxiliary DNA-binding determinant

Protein binding to DNA was tested using a radioactively labeled optimized HiNF-P binding site oligonucleotide by electrophoretic mobility shift assay (EMSA). (A) Binding of wild type or ΔPSCR mutant HiNF-P proteins overexpressed in HeLa cells was tested by EMSA using nuclear extracts. Wild type HiNF-P forms a distinct protein/DNA complex (lane 2; grey arrowhead); a non-specific band (ns; open arrow head) is also observed; competition experiments with specific wild type (P; lane 3) or mutant (Pm; lane 4) unlabeled oligonucleotides were performed at 100-fold molar excess. The ΔPSCR HiNF-P mutant lacks the ability to bind to the HiNF-P binding site (lane 5). The sub-cellular localization and equivalence of expression levels for wild type (lane 2) and ΔPSCR mutant (lane 3) HiNF-P proteins were confirmed by western blot (lower panel; CDK2 is shown as loading control) using FLAG antibody (ns: non-specific). (B) EMSA with recombinant wild type and mutant

NIH-PA Author Manuscript

NIH-PA Author Manuscript

NIH-PA Author Manuscript

HiNF-P proteins produced by a coupled in vitro transcribed/translated (IVTT) system. Recombinant wild type HiNF-P binds to its recognition binding site to form a single protein/DNA complex band (lane 3). Specificity was assessed by competition with specific wild type (P; lane 4), mutant (Pm; lane 5) or non-specific (ns; lane 6) unlabeled oligonucleotides at a 100-fold molar excess. The external deletion mutants 1−452 (lane 7) and 1−395 (lane 8) are both capable of binding to a HiNF-P element, although the 1−395 mutant exhibits decreased binding activity (compare lane 8 with lane 3). (C) EMSA with IVTT-produced wild type (lane 1) and ΔPSCR deletion (lanes 2−6) HiNF-P proteins. The recombinant mutant proteins ΔPSCR (lane 2), ΔPSCR1 (lane 3) and ΔPSCR4 (lane 4) do not bind to HiNF-P binding motif, while the mutants ΔPSCR2 (lane 5) and ΔPSCR3 (lane 6) remain competent for binding. Recombinant wild type and mutant proteins were all produced at comparable levels, as demonstrated by western blot analysis using FLAG antibody (lower panel; ns: non-specific). (D) EMSAs with IVTT-produced $p220^{NPAT}$ together with wild type (lanes 1−4) and mutant HiNF-P proteins (lanes 5−12). We tested external 1−452 (lanes 5 and 6) and 1−395 (lanes 7 and 8) and internal ΔPSCR2 (lanes 9 and 10) and ΔPSCR3 (lanes 11 and 12) HiNF-P deletion proteins. Ternary $p220^{NPAT}$/HiNF-P/DNA complex formation was assayed by combining HiNF-P proteins with (lanes 3, 4, 6, 8, 10 and 12) or without (lanes 1, 2, 5, 7, 9 and 11) an N-terminal segment of $p220^{NPAT}$. Specificity of complex formation was assessed by competition with 100-fold excess of unlabelled HiNF-P DNA oligonucleotide (lanes 2 and 4). Depicted on the left are the positions of the HiNF-P/DNA and $p220^{NPAT}$/HiNF-P/DNA complexes. Gels were overexposed to enhance the ternary complex visualization.

NIH-PA Author Manuscript

NIH-PA Author Manuscript

NIH-PA Author Manuscript

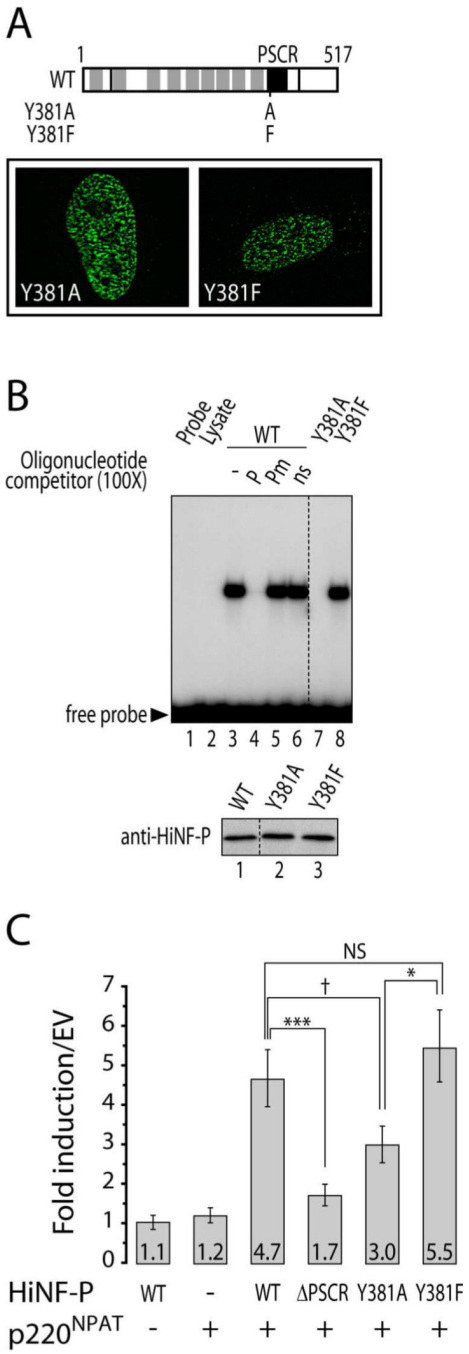

Figure 5. Mutation of tyrosine 381 within the PSCR motif of HiNF-P abolishes its DNA-binding activity

(A) Nuclear localization of point mutants Y381A and Y381F of HiNF-P was established by immunofluorescence in human U-2 OS cells as described in Figure 3. The top portion shows a diagram of HiNF-P and the position of the mutated tyrosine within the PSCR (for further details see Fig. 1B and Fig. 6). (B) EMSA with recombinant wild type and point mutant HiNF-P proteins produced by coupled IVTT. Recombinant wild type HiNF-P binds to its recognition element to form a single protein/DNA complex band (lane 3). Specificity was assessed by competition with specific wild type (P; lane 4), mutant (Pm; lane 5) or non-specific (ns; lane 6) unlabeled oligonucleotides at a 100-fold molar excess. Mutation of tyrosine 381 to alanine

NIH-PA Author Manuscript

NIH-PA Author Manuscript

NIH-PA Author Manuscript

(lane 7) but not to phenylalanine (lane 8), abolishes binding of HiNF-P to its cognate binding site. Recombinant wild type (lane 1) and point mutant (lanes 2 and 3) proteins were all produced at comparable levels as demonstrated by western blot analysis using FLAG antibodies (lower panel). (C) HiNF-P-depleted U-2 OS cells were transfected with a H4/n-Luc construct together with expression vectors for wild type HiNF-P (WT), mutant Y381A or Y381F and $p220^{NPAT}$ for 24 h. Basal levels are observed when $p220^{NPAT}$ is transfected alone. Transfection of exogenous wild type HiNF-P together with $p220^{NPAT}$ produces a 4.7-fold co-activation; however the co-transfection of mutant ΔPSCR and $p220^{NPAT}$ is incapable of co-activation. The Y381A mutation but not the Y381F mutation decreases the transactivation potential of HiNF-P and $p220^{NPAT}$ on the histone H4 promoter. Results are presented as mean ± standard error. NS: not significant, †: $0.05<p<0.1$, *: $p<0.05$, **: $p<0.01$ and ***: $p<0.001$.

NIH-PA Author Manuscript

NIH-PA Author Manuscript

NIH-PA Author Manuscript

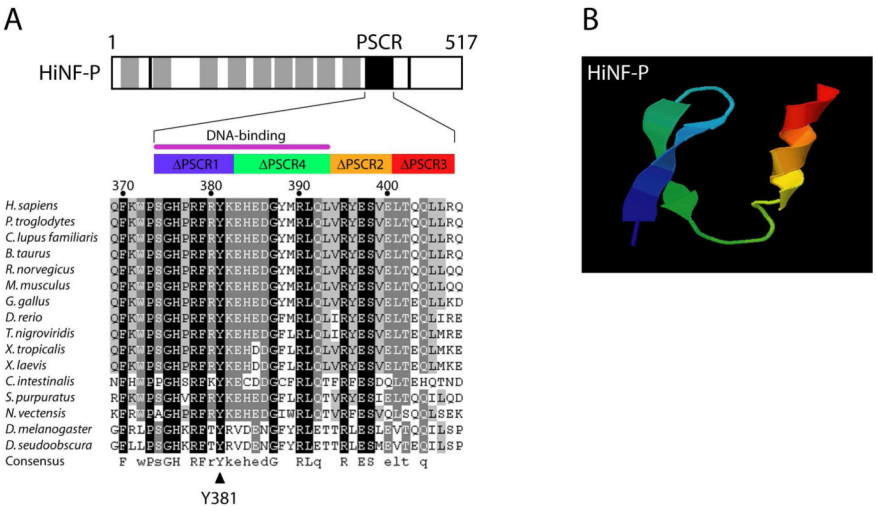

Figure 6. The PSCR motif of HiNF-P is conserved throughout evolution

(A) Multiple sequence alignment of the PSCR region of human HiNF-P with the corresponding amino acid residues from different metazoan species. Alignments were performed with ClustalW and GeneDoc. Black, dark and light gray shades represent 100%, 80−95%, and 60−75% of conservation, respectively. Conserved residues within a putative consensus sequence of the PSCR are shown below the alignment. The purple line above the diagram shows the part of the PSCR required for DNA-binding and the closed arrow head at the bottom shows a residue critical for the DNA-binding activity of HiNF-P. (B) Molecular modeling of the PSCR of human HiNF-P was done using 3D-Phyre (40,41). Colored regions correspond to the PSCR segments in the diagram in (A).